

Estimates of the information provided by GPS slant data observed in Germany regarding tomographic applications

M. Bender,¹ G. Dick,¹ J. Wickert,¹ M. Ramatschi,¹ M. Ge,¹ G. Gendt,¹ M. Rothacher,¹ A. Raabe,² and G. Tetzlaff²

Received 20 August 2008; revised 12 December 2008; accepted 23 December 2008; published 21 March 2009.

[1] The observation of GPS slant delays from ground GPS networks can be used to reconstruct spatially resolved humidity fields in the troposphere by means of tomographic techniques. Tomography is always related to the solution of inverse problems which are very sensitive to the quality of the input data. Prior to a tomographic reconstruction, it is therefore necessary to quantify the information provided by a given set of GPS slant delay data. This work describes the properties and the information content of more than two million GPS slant delays taken in March 2006 by a continuously operating German GPS network. The temporal and spatial distribution of the slant paths in the atmosphere and their angular distribution in the local system of the GPS station is given. These distributions depend on the satellite orbits and show some characteristic pattern. The available information is estimated by investigating the distribution of intersection points between the slant paths. From these data it is possible to identify regions that are well covered by GPS slant paths and to evaluate the applicability of the existing German GPS stations for continuous atmosphere sounding.

Citation: Bender, M., G. Dick, J. Wickert, M. Ramatschi, M. Ge, G. Gendt, M. Rothacher, A. Raabe, and G. Tetzlaff (2009), Estimates of the information provided by GPS slant data observed in Germany regarding tomographic applications, *J. Geophys. Res.*, 114, D06303, doi:10.1029/2008JD011008.

1. Introduction

[2] Research activities in the field of climate change and atmospheric processes increased in the last years. Efforts have been made to get a deeper insight into the basic processes and to refine the numerical weather models. An essential condition for a better understanding of atmospheric processes is the availability of spatially resolved observations. Especially the next generation of high-resolution weather models requires highly resolved input data and additional observations for the model validation.

[3] The upcoming methods of GPS meteorology [Bevis *et al.*, 1992; Businger *et al.*, 1996; Ware *et al.*, 1997] are very promising to provide atmospheric humidity information on the whole scale from local observations [Gendt *et al.*, 2004] to a global ground- and space-based monitoring [Heise *et al.*, 2006; Wickert *et al.*, 2007, 2008, 2009]. Deficiencies in the precipitation forecast lead to a special demand for spatially resolved humidity observations on the scale of regional numerical weather prediction models. The assimilation of spatially resolved humidity fields or the GPS slant delays leads to an improved internal state of the weather

model which should result in better forecasts [Zus *et al.*, 2008]. Such temporally and spatially resolved fields can be obtained from the GPS tomography which reconstructs the spatial atmospheric structures from a large number of GPS observations. Numerous field campaigns demonstrated the great potential of this method [Seko *et al.*, 2000; Ware *et al.*, 2000; Flores *et al.*, 2001; Gradinarsky and Jarlemark, 2004] and a first nationwide GPS tomography system has already been established in Switzerland [Troller *et al.*, 2006b]. Currently, several national GPS networks reach a receiver density which is sufficient for first tomographic studies.

[4] The basic GPS quantity required to obtain spatially resolved information about the atmosphere is the slant total delay (STD), i.e., the path delay of the GPS signal due to the neutral atmosphere. The STD depends on the refractivity N of the atmosphere as

$$STD = 10^{-6} \int_S N(s) ds, \quad (1)$$

where S is the curved raypath of the signal through the atmosphere and $N(s)$ is the refractivity ($N = 10^6 (n - 1)$; n refractive index of air) along this path [Bevis *et al.*, 1992]. The refractivity depends on the pressure, the temperature and the humidity. If it is possible to reconstruct the atmospheric refractivity field N from the slant delays one can in principle receive information about at least one of these quantities. To

¹Helmholtz-Zentrum Potsdam, Deutsches GeoForschungsZentrum, Potsdam, Germany.

²Institut für Meteorologie, Universität Leipzig, Leipzig, Germany.

obtain the humidity information the slant wet delay (SWD) due to the water vapor in the troposphere must be separated. This is usually done by estimating the slant hydrostatic delay (SHD), for example, with the Saastamoinen model and assuming $SWD = STD - SHD$. Refraction of the GPS signal in the atmosphere leads to bending angles up to 1° at very low elevations and the raypath S is in general not a straight line. The GPS radio occultation technique utilises the ray bending to derive vertical profiles of several atmospheric quantities [Kursinski *et al.*, 1997]. In this work only the spatial coverage of the atmosphere by the GPS signal paths is considered. The small deviations of the real curved path from a straight line, i.e., the ray bending, can be neglected as only the geometric aspects are discussed.

[5] Each single path delay provides only one integral value which corresponds to the refractivity distribution along the raypath from the GPS satellite to the GPS station. To obtain a spatially resolved refractivity field a large number of path delays which cover large parts of the atmosphere from a wide angular range must be combined. Such a task where the internal state of a system has to be reconstructed from external observations defines an inverse problem. Inverse problems are very often underdetermined and ill-posed. The solution, if any exists, may not be unique and may not be stable; that is, very small variations in the observations may lead to an entirely different reconstructed state. The solution of such problems is usually referred to as tomography. A large number of tomographic techniques exists for different applications [Kak and Slaney, 1999; Natterer, 2001]. The GPS tomography has to deal with the special geometry given by a small number of GPS satellites in their orbits and, compared with the volume of the troposphere, a rather small number of GPS ground stations. The currently available GPS networks have not been designed for meteorological applications and cannot provide a complete data set for tomographic reconstructions, as, for example, tomographs developed for medical applications or nondestructive material tests.

[6] The GPS tomography has always to solve an ill-posed inverse problem with incomplete input data. The incompleteness describes the fact that usually not the whole volume, i.e., the troposphere, is covered by a sufficient number of slant paths from a wide angular range. Reconstruction techniques rely therefore on additional data or model constraints to fill these gaps and to obtain a complete 3D field. The reconstruction shows in this case not only the information from the GPS data but also features of the tomographic technique and the extra information and constraints used. The spatial distribution and especially the vertical profiles may, at least in some regions, be an “artifact” of the specific reconstruction technique. Therefore, it is important to investigate the information provided by a given data set of slant delays prior to the reconstruction and to evaluate the results of the tomography accordingly.

[7] The characteristics of the slant data derived from the German GPS stations in March 2006 were investigated in this work regarding future tomographic reconstructions. An attempt was made to select some features of the GPS slant data which are of high relevance for the spatial reconstruction of the humidity field and to quantify the information contained in the data, continuing a preceding study which was based on simulated slant data [Bender and Raabe,

2007]. Some of the basic properties are the number of slant data available at a certain time and the spatial distribution of the slant paths in the troposphere, especially their frequency distribution with respect to the azimuth and the elevation. These results give a first impression of the spatial coverage. The information is estimated by investigating the temporal and spatial distribution of intersection points between different slant paths. The existence of intersections in a certain region is a necessary condition to localise the information and their distribution represents the available information in a much more realistic way than the density of slant paths. This study is mainly based on the geometrical properties of the slant paths, i.e., a set of straight lines and their intersections. The slant delay, i.e., the path delay due to the wet atmosphere, has so far not been considered. All data presented here were observed in the first 3 days of March 2006.

2. Characteristics of the Slant Data

[8] The GPS data were analyzed in near real time (NRT) by the GFZ processing centre using the GFZ EPOS software [Gendt *et al.*, 1999a], which is based on a least squares adjustment of undifferenced phase measurements and is also applied by the International GNSS Service (IGS) Analysis Centre at the GFZ [Gendt *et al.*, 1999a, 1999b]. The analysis uses hourly GPS data sampled with 30-s temporal resolution. Owing to the steadily increasing number of sites an analysis strategy was developed on the basis of the “Precise Point Positioning” (PPP) method [Zumberge *et al.*, 1997] with processing of each site separately. This approach allows the parallel processing of the data on different processors and/or computers to guarantee in-time data processing under varying conditions.

[9] There are several GPS network providers which operate GPS stations in Germany. The most dense networks belong to the German satellite positioning service (SAPOS) and the Federal Agency for Cartography and Geodesy (BKG), which operate in total more than 260 stations. Additional GPS observations can be obtained from international providers like IGS and the IAG Reference Frame Sub-Commission for Europe (EUREF) and some stations are operated by the GFZ itself. Although some stations are used jointly by several services the total number of German GPS stations exceeds 300. The GFZ collects most of these data operationally and makes efforts to integrate them into its NRT processing. In this work only the ~ 135 stations are considered which were part of the NRT processing in March 2006.

[10] The NRT GPS data processing results in tropospheric products which are available from GFZ and are especially relevant for meteorological applications, i.e., the integrated water vapor (IWV) and the STD. The IWV is based on all data sampled by a given station in a given period. All these data are combined to obtain the most reliable zenith total delay (ZTD). The ZTD is closely related to the IWV and the precipitable water vapor above the GPS station [Bevis *et al.*, 1994; Dick *et al.*, 2001]. The STDs are processed in the following way. Each STD represents a different view through the atmosphere, i.e., the raypath from a GPS satellite to the GPS receiver. The individual GPS observations are processed separately and the path delay is determined from only one

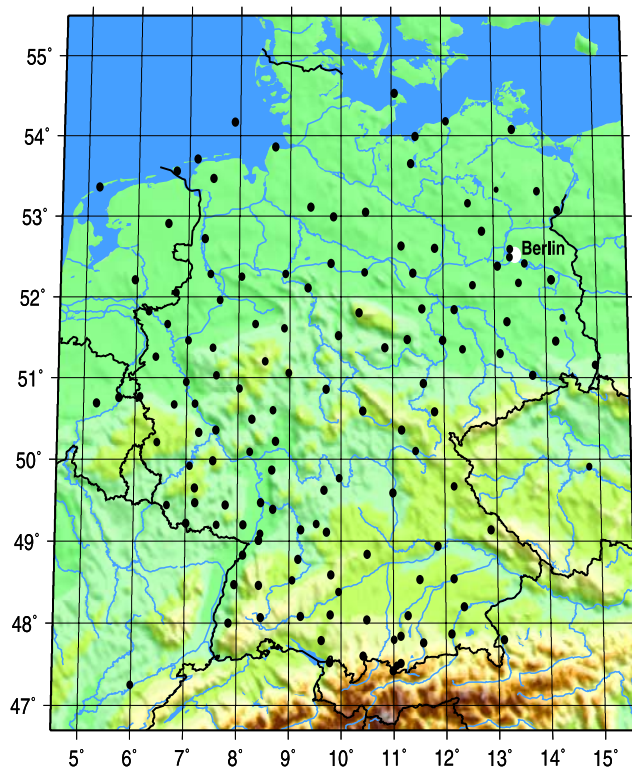


Figure 1. Map of the 135 GPS ground stations available in March 2006. The data from several network providers, for example, SAPOS, IGS, BKG, and GFZ, are collected at the GFZ and processed in near real time.

GPS observation. This results in a large number of STD values as each station provides as many STDs at a given time as GPS satellites are visible.

[11] Currently, GFZ analyses the IWV data with a temporal resolution of 15 min and STD data with a resolution of 2.5 min. Every station provides one IWV quantity and approx. 48 STD values within a period of 15 min. In March 2006 the data from 135 stations in Germany and neighbored countries were processed operationally by the GFZ (Figure 1). The IWV data provided by this network give a good representation of the total amount of water vapor and its horizontal distribution above Germany. The vertical humidity profiles cannot be obtained from the IWV but it is possible to obtain spatially resolved humidity fields from the STD data.

[12] The station data are operationally collected at the GFZ and should be available every hour with a delay of 10–15 min. In reality, the data can be delayed or lost for several reasons, for example, hardware failures or network problems. How many data are available for a given application depends on the specific requirements. In real-time applications, delayed data cannot be used while user of postprocessed data will get the maximum quantity. The network availability is therefore a key factor which has to be considered for tomographic applications running in near real-time mode. In this work, postprocessed data were used; 96.8% of the data were available for the 3 days regarded in this work where some stations had data gaps on the third day (92.9%) but almost no failures on the first (98.7%) and

second (98.8%) day. This explains the slightly decreasing number of slants on the third day shown in Figure 2.

[13] The GPS stations in Germany are rather inhomogeneously distributed with distances between neighbored receivers varying between ~ 7 km and ~ 85 km. On average the closest station is 37 km afar, at least 3 stations can be found within a radius of 59 km and 6 stations within 82 km. The entire network provides $\sim 800,000$ slant delays per day. The number of observations available within a period of 15 min (Figure 2) varies between ~ 4400 and ~ 8150 with a mean value of ~ 6200 . Regarding tomographic applications a large number of slant paths propagating through many horizontally neighbored grid cells would be desirable to get a good vertical resolution. This number depends on the slant paths' elevation and the grid spacing as well (Figure 3). The grid used for the tomographic reconstructions based on the German GPS stations might have a horizontal resolution of 50 km to 60 km. The fraction of slant paths propagating through more than one vertical column of the grid can be estimated from geometric considerations if a random distribution of stations inside the grid is assumed. Approximately two thirds of the slants within a 60 km grid would reach a neighbored cell and an elevation $\varepsilon \geq 46^\circ$ would be required (see Figures 2 and 4a). However, only a much smaller fraction of the slant paths with elevations below $\sim 15^\circ$ covers a large distance within the lower part of the atmosphere and would provide information about the most important part of the water vapor distribution. As can be seen in Figure 2 the available slant paths with $\varepsilon \leq 46^\circ$ show variations between ~ 2000 and ~ 6000 observations. Fast fluctuations of more than 50% are possible within less than 1 h.

[14] The distribution of elevation angles within 3 days in March 2006 is given in Figures 4a and 4c. The 2D histogram shows the temporal variation of this distribution with a resolution of 15 min and 2° . The accumulated data from 1,770,747 observations result in the 1D histogram shown above. This distribution has some characteristics which are almost ideal for tomographic applications. The

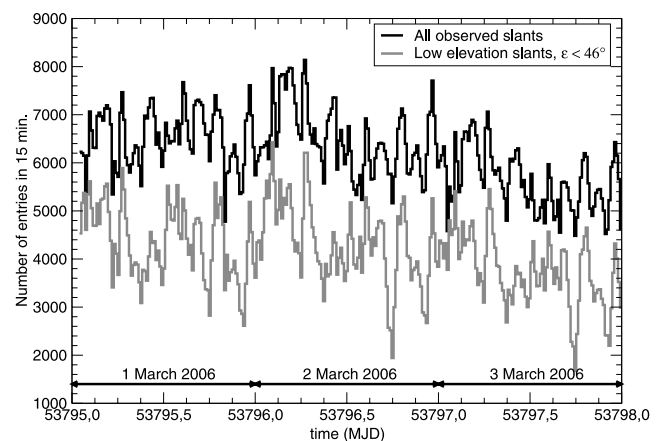


Figure 2. Number of slants available within 15-min periods. The number of slants with elevation angles below $\varepsilon \leq 46^\circ$ (grey) amount to approximately two thirds of the total number of slants (black). These “flat” slants will most probably propagate to at least one horizontally neighbored cell. An elevation cutoff angle of 7° was used.

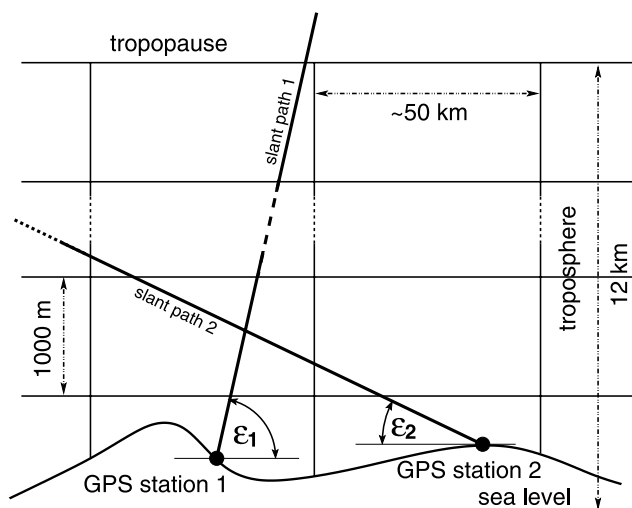


Figure 3. Slant paths with different elevations ε propagating through a spatial grid.

maximum is close to the elevation cutoff angle $\varepsilon_{\min} = 7^\circ$ providing maximum information in the atmospheric boundary layer, i.e., the lowest part of the troposphere up to ~ 1 km which contains the highest concentration of water vapor. The decreasing number of slant paths with higher elevations has little effect on tomographic applications as each “flat” slant path intersects with a large number of “vertical” slant paths. The total number of intersections depends therefore mainly on the “flat” slant paths.

[15] The distribution of elevations within a given period depends strongly on the satellite constellation and the period within the slant data can be accumulated. The shape of the distribution changes significantly if only a short period is regarded, for example, 15 min as in Figure 4c. There are periods with a large number of “flat” slant paths but also periods where almost no observations with low elevations are available.

[16] The temporal distribution of the azimuth angles and the corresponding accumulated distribution are given in Figures 4b and 4d. The distribution shows some preferred directions of the slant paths’ azimuth. Slants pointing south, in northeastern or northwestern direction occur with a higher probability. The temporal variation of this distribution is not as pronounced as for the elevation. Three peaks can clearly be identified for all times only their position varies slightly with time (Figure 4d). This feature leads, together with the nearly random distribution of GPS stations, to highly variable temporal distributions of intersection points.

[17] Furthermore, the azimuth and the elevation of the slants is highly correlated (Figures 4e and 5). Slants with low elevations observed in Germany (latitude 47° – 55°) point mainly in the northeastern and the northwestern direction. As discussed in the next section it would be desirable to have as many intersections with slants of neighbored stations as possible. This could most easily be achieved if neighbored stations were placed in a direction where a large number of slants with low elevations could be expected. An increasing number of observations in the lower part of the troposphere would follow. In this case, slants with an elevation of 7° could intersect with an almost

vertical slant path from a neighbored station 30 km away at an altitude of ~ 4 km [Bender and Raabe, 2007]. The slant paths pointing south show no preferred elevation. The distributions shown in Figures 4b, 4d, and 4e depend significantly on the latitude of the observation point. The azimuth distribution is almost flat at high latitudes ($\varphi > 80^\circ$) or shows four peaks at approximately $\varphi = 30^\circ, 150^\circ, 210^\circ, 330^\circ$ near the equator.

[18] These features follow directly from the shape of the satellite orbits as observed in the local horizon system [Santerre, 1991]. Considering northern latitudes between 47° and 55° the satellites rising or setting in the North appear in a rather limited region of azimuth angles (Figure 5). As a consequence satellites with low elevation angles accumulate in these regions. The azimuth and elevation angles of satellites rising or setting in the south are much more evenly distributed.

3. Preconditions to GPS Water Vapor Tomography

[19] The GPS water vapor tomography makes use of the humidity information contained in the slant delay data and reconstructs the spatial distribution of the humidity in the troposphere from a large number of slant delays [Flores et al., 2001; Troller et al., 2006a]. The quality of the reconstructed fields depends strongly on the information provided by a given slant data set. It can be expected from the results of the previous section that the information changes significantly with time. Therefore, criteria are required to quantify the information content of the slant data. One possibility is to investigate the distribution of intersection points between different slants [Bender and Raabe, 2007]. The slant delay is a quantity which is integrated along the slant path. Regarding only one slant path it is not possible to subdivide this quantity along its path. A large number of intersecting slants which cover a wide angular range is required to locate the information. Because of the significance of these intersection points one can regard the density of the intersection points as an estimation of the information density provided by a given data set.

[20] To use the present information in an optimal way it is necessary to adjust the parameters of the tomographic reconstruction to the available data. The most important parameters are the period within the slant data are accumulated and the spatial resolution of the chosen tomography grid.

3.1. GPS Tomography

[21] The spatiotemporal information contained in a given data set is obviously independent from the reconstruction technique used to recover that information. This work is an attempt to quantify the information content without any reference to a specific technique. However, the problems appearing during the tomographic reconstruction process are mentioned several times and a short description of the tomographic technique used is given.

[22] The basic inversion problem appearing in GPS tomography [Flores et al., 2001; Troller et al., 2006b; Kunitsyn and Tereshchenko, 2003] can be described by

$$Ax = m, \quad (2)$$

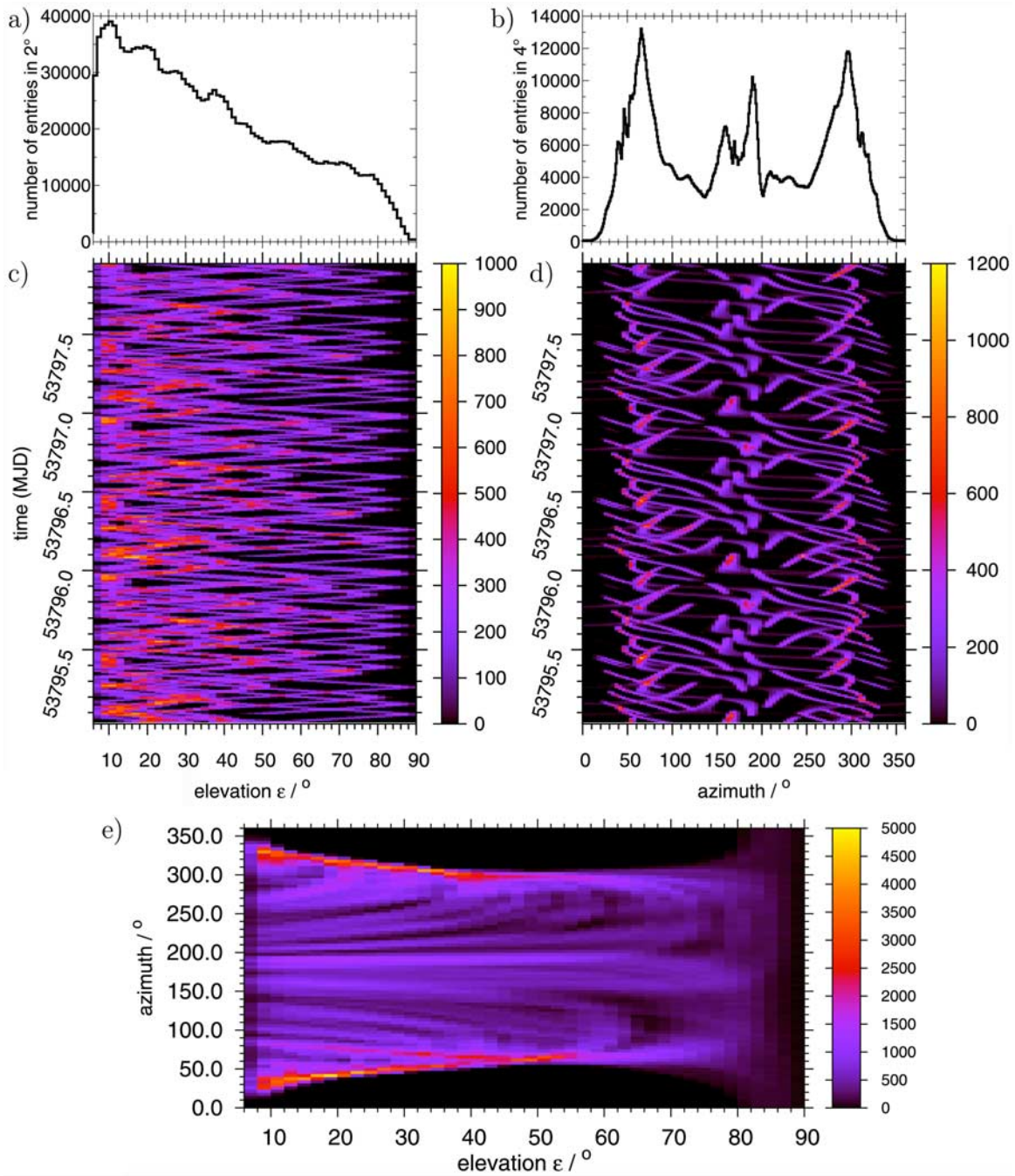


Figure 4. Elevations (a, c) ε and (b, d) azimuth of the slants collected within 3 days. The temporal variation of the elevation (Figure 4c) is given with a resolution of 2° in ε and 15 min. Figure 4a shows the accumulated distribution of the 3 days. The temporal variation of the azimuth distribution (Figure 4d) is given with a resolution of 4° and 15 min. Figure 4b was accumulated over 3 days. (e) The correlation of slant path elevation with the azimuth direction. The color code indicates the number of entries within each histogram bin.

where \mathbf{m} is the vector of observations, i.e., the slant delays, \mathbf{x} is the unknown state vector representing the refractivity of the atmosphere and \mathbf{A} is the kernel matrix. \mathbf{A} is a large sparse matrix defined by the spatial grid used to discretise the atmosphere and the start and end points of the raypaths. The matrix elements a_{ij} are given by the subsection of the i th raypath inside the j th grid cell. As each raypath propagates only through a limited number of cells of a large

3D grid most of the a_{ij} are zero. A wealth of techniques [Kak and Slaney, 1999; Natterer, 2001] has been developed to solve such problems but only computational efficient algorithms can be applied to the GPS tomography. Depending on the spatial resolution the state vector \mathbf{x} has a dimension of $\sim 2500 \dots \sim 12000$ and the number of observations is in the range of ~ 5000 to $\sim 30,000$ for reconstruction periods between 15 and 60 min.

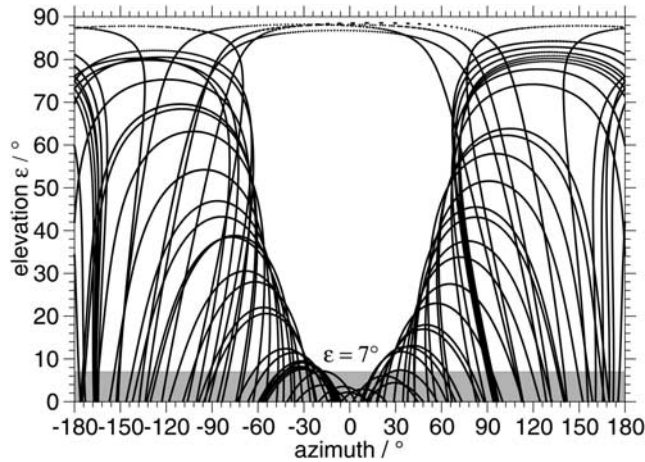


Figure 5. Tracks of the GPS satellites in the local horizon system of the GPS stations. These tracks depend considerably on the latitude of the GPS stations. All stations regarded here are located between northern latitudes of 45° and 55°. The elevation cutoff angle was 7°.

[23] The family of algebraic reconstruction techniques (ART) [Subbarao et al., 1997; Kunitsyn and Tereshchenko, 2003] provides fast algorithms which lead to stable results. These iterative techniques process the matrix A row by row and no matrix inversion is required. The multiplicative algebraic reconstruction technique (MART) was chosen because it leads to the most reliable results with the smallest number of iterations [Stolle et al., 2006],

$$x_j^{k+1} = x_j^k \cdot \left(\frac{m_i}{\langle A^i, x^k \rangle} \right)^{\frac{\lambda m_i^j}{\sqrt{\langle A^i, A^i \rangle}}} \quad \text{with } j = 1, \dots, N. \quad (3)$$

[24] The subscript j denotes the grid cell, i the observation and k the iteration step, the vector A^i is the i th row of the matrix A containing the path length of the i th raypath in all N grid cells, and λ is the relaxation parameter.

[25] The tomographic reconstruction starts with an initial field x^0 of the atmospheric refractivity. This field is taken from an analysis of a numerical weather model (COSMO-

EU) which should be rather close to the real state. The start field is refined by the MART algorithm until the difference δ between the back projection $m^k = Ax^k$ and the observations m^0

$$\delta = \frac{1}{I} \sum_{i=1}^I (m_i^k - m_i^0) \quad (4)$$

becomes minimal which is usually the case after 50...200 iterations. A relaxation parameter $\lambda = 0.2$ was chosen. The quality of the reconstructed field x^k depends on the quality of the initial field and the data.

3.2. Total Number of Intersection Points

[26] The computation of intersection points in three dimensions requires the specification of some minimum distances between a pair of slants. Two slants do hardly ever intersect geometrically in three dimensions, i.e., have a common point. But it is always possible to compute the minimum distance between any pair of slants. Two slants can be regarded as “intersecting” if the minimum distance is below some threshold value. The number of intersection points depends therefore considerably on the chosen threshold value. The thresholds were chosen in analogy to the grid spacing, for example, 50 km horizontally and 1 km vertically as in Figure 6 (right). The uppermost level is given by the tropopause which defines the upper limit of the troposphere at a height of ~ 12 km. As virtually all atmospheric water vapor is contained in the troposphere altitudes above 12 km are usually not regarded by the GPS water vapor tomography.

[27] The total number of intersection points depends also on the temporal resolution, i.e., the duration of the selected observation period which will result in one single tomographic reconstruction. The temporal variation is due to the varying number of available slants and the satellite constellation.

[28] The geometry of the reconstruction area requires a rather asymmetric grid with a horizontal spacing of ~ 50 km and a vertical spacing of ~ 1 km. Most of the slant paths with a horizontal distance below 50 km will in this case be rejected because their vertical spacing is larger than 1 km.

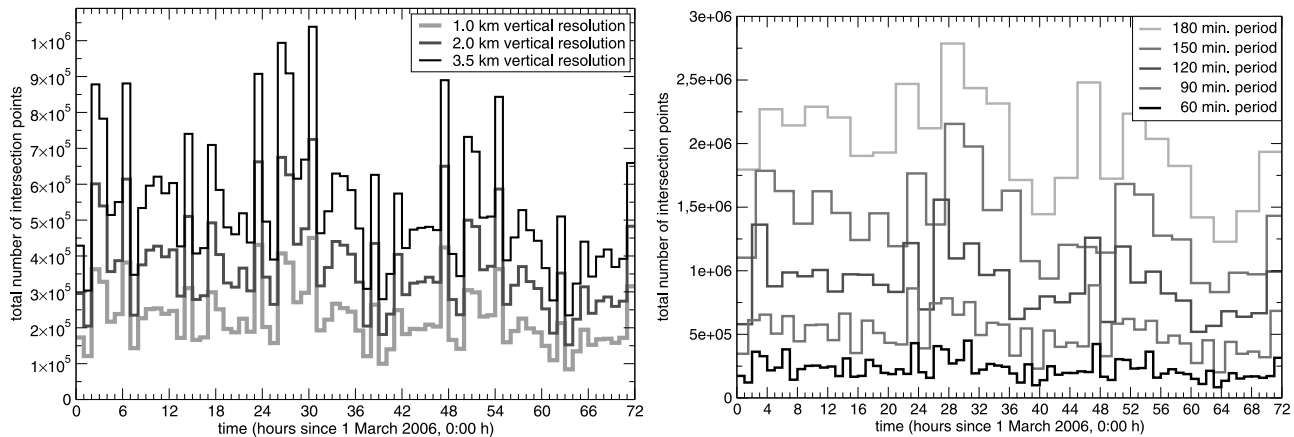


Figure 6. Total number of intersection points between the slant paths: Variation of (left) the vertical distance and (right) different sampling periods. The horizontal resolution is 50 km in both cases. A period of 1 h was chosen in the left graph and a vertical resolution of 1 km in the right one.

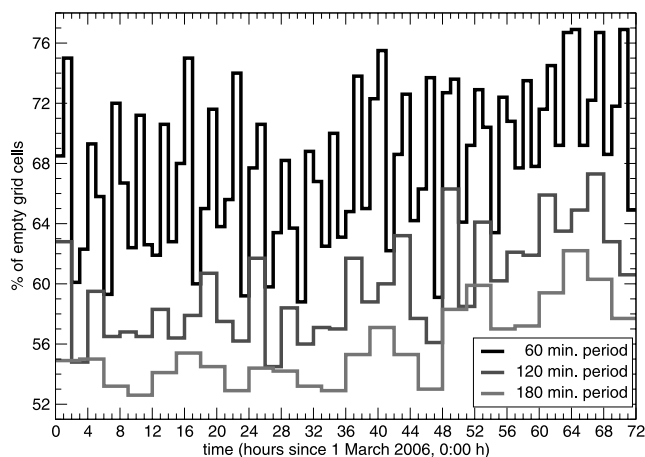


Figure 7. Percentage of empty grid cells: The intersection points were computed using 50-km horizontal spacing and 1-km vertical spacing. Slants from periods varying from 60 min to 120 and 180 min were used.

Variations of ± 20 km in the horizontal spacing have under these conditions little effect on the number of intersection points. In contrast, the vertical spacing can change the available intersection points by a factor of 2 or 3. Figure 6 (left) shows the time series of all intersection points computed for a vertical grid spacing of 1, 2 and 3.5 km and a horizontal spacing of 50 km. The available intersections increase rapidly with the vertical spacing but as most of the water vapor is located in the lower troposphere, resolutions below ~ 2 km become meaningless.

[29] A similar effect can be obtained by enlarging the sampling period (Figure 6, right). The number of intersection points increases exponentially with the number of available slants, for example, on average from $\sim 250,000$ (60 min) to $\sim 975,000$ (120 min) and $\sim 2,125,000$ (180 min). This increases the spatial resolution at the expense of the temporal resolution. It depends on the application which temporal resolution is required. The sampling period must in any case be chosen sufficiently short so that most of the air remains in the same grid cell. Owing to advection the air moves through the grid and it depends on the wind speed how long the atmosphere might be regarded as stationary.

[30] Tomographic applications require not only a large number of intersection points but also a rather homogeneous spatial distribution which guarantees a minimum of information in each cell. The total number of “empty” cells with no intersection points at all is therefore a critical parameter. While the surface layer could be filled with meteorological observations and the topmost layer might be preset to some reasonable small value there is little information which can be used to fill gaps inside the reconstruction volume. The number of empty cells should therefore not exceed the number of boundary cells of the tomography grid. As can be seen in Figure 7 the number of “empty” cells is well above 50%. This number cannot significantly be reduced even if one goes down to rather poor spatial and temporal resolutions.

3.3. Distribution of Intersection Points

[31] A large fraction of the atmospheric water vapor is located in the boundary layer. It is therefore essential to

reconstruct the lower part of the troposphere reliably. One precondition is the existence of intersection points in this region. Unfortunately, the vertical distribution of intersection points has its minimum in the lower troposphere (Figure 8). The shape of the distribution does not change significantly with time or with the spatial resolution used to compute the intersection points. The number of intersection points below 2000 m remains very small even if a low spatial resolution is chosen and data from a rather long period are collected. However, the total number of intersections changes significantly as could be expected from Figure 6. Most of the vertical distributions (71%) fall within the shaded region of Figure 8 but the information obtained in the “best” and the “worst” case (see Figure 8, 2 March 2006, 0600 UTC, and 3 March 2006, 1500 UTC) differs notably and will lead to a varying quality of the reconstructed humidity fields. In these 3 days 17% of the distributions were rather flat with a low number of intersection points which do not significantly increase at higher altitudes. Twelve percent show a high number of intersections which outnumber the average distribution even at low altitudes.

[32] For certain satellite constellations there appears a peak near the surface layer ≤ 500 m in Figure 8. This peak is due to the rather dense cluster of GPS stations around Berlin ($52^\circ 31'N$, $13^\circ 25'E$; Figures 1, 9b, and 9d). This leads occasionally to a large number of intersections in the lowest layer but usually (shaded region in Figure 8) there are only very few intersections below 1000 m. These peaks form a rather high concentration of intersections within several grid cells. Such a distribution does not provide any vertical information but may destabilize the reconstruction process. However, the high density of intersection points near such a cluster of stations indicates that a dense GPS network would provide valuable information about the boundary layer if its horizontal extension would be sufficiently large.

[33] A reliable tomographic reconstruction would not only require a large number of intersecting slants but also slants from a wide angular range. As can be seen in

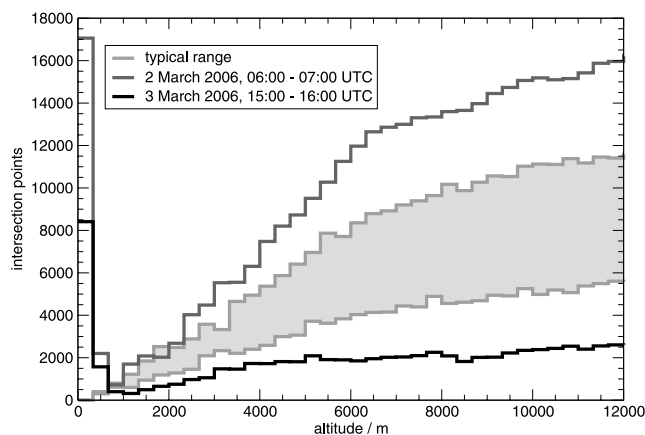


Figure 8. Vertical distribution of intersection points found with a horizontal distance ≤ 50 km and a vertical distance ≤ 1 km. The “best” (2 March 0600 UTC) and the “worst” (3 March 1500 UTC) distribution is shown. Most of the distributions (71%) fall within the scope of the shaded region, 12% are better, and 17% are worse.

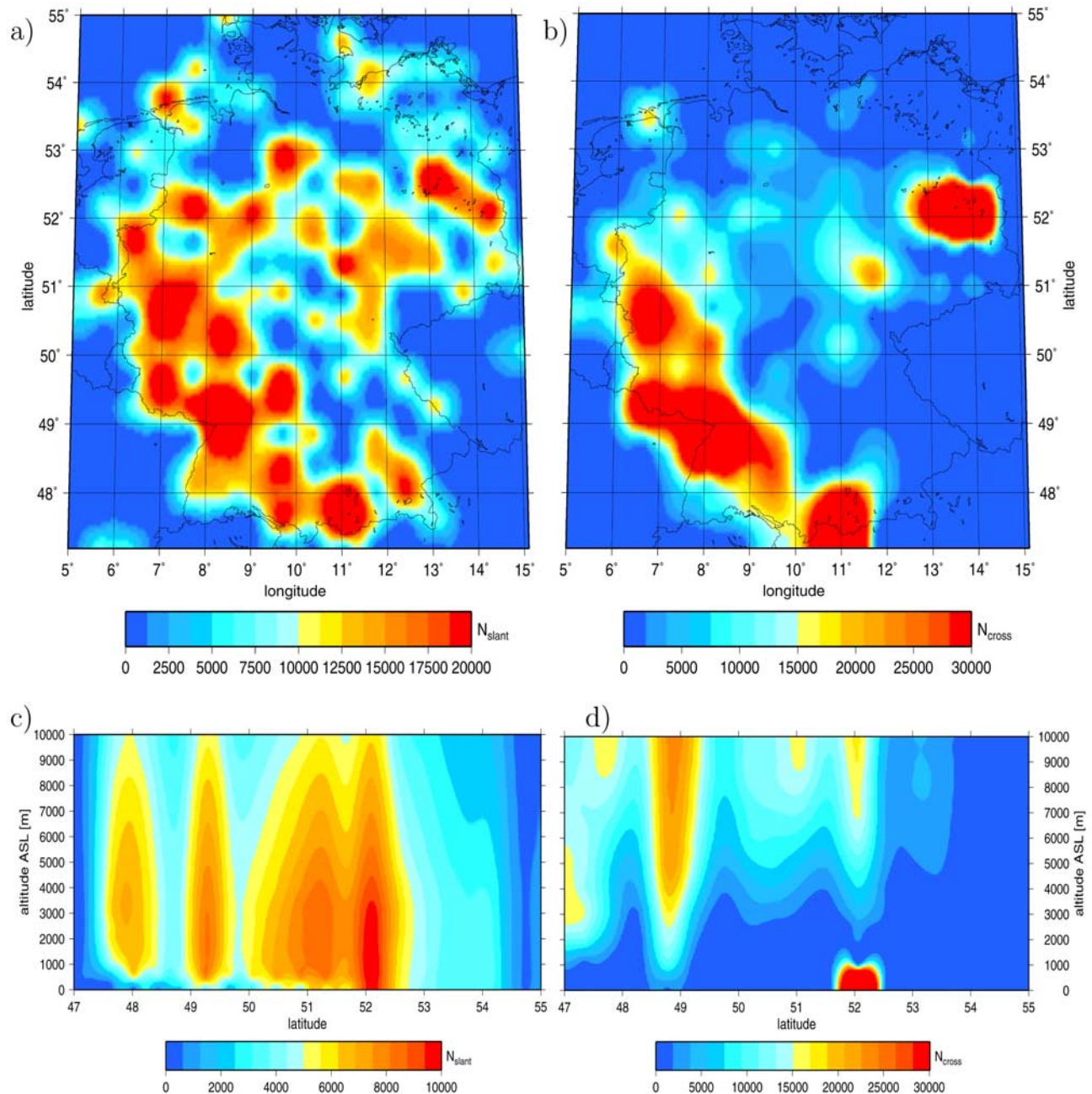


Figure 9. (top) Horizontal and (bottom) vertical distribution of (left) the slant paths and (right) the intersection points. (b) The horizontal projection of the intersections per voxel shows a much more clustered structure than (a) the slant paths per voxel. A large number of slant paths can be found in (c) the lower troposphere but only few intersections as given by (d) the vertical projection along the N-S axis. N_{slant} and N_{cross} are the total numbers of entries within a vertical column of the grid in case of the horizontal projection and within an E-W column in case of the vertical projection.

Figure 10 most slants show crossing angles between 30° and 150° , i.e., are far from being parallel or antiparallel. The distributions shown in Figure 10 are typical: There is a large number of cases with a normal distribution (0500 UTC) or a rather flat distribution (0800 UTC). Some constellations lead to pronounced maxima at certain angles (0200 UTC) which are usually not far from 90° . Another typical feature is the asymmetry which leads to an increased number of crossing angles between $\sim 120^\circ$ and $\sim 160^\circ$ indicating slant

paths from opposite directions which intersect at rather low elevations. Altogether, it can be expected that slants from a wide angular range intersect in most parts of the grid which are covered by slants.

[34] One of the most important features of a slant data set is the spatial distribution of the slant paths and their intersection points. It is obvious that no information can be obtained in regions with no slant data at all. But a large density of slants without an adequate number of intersec-

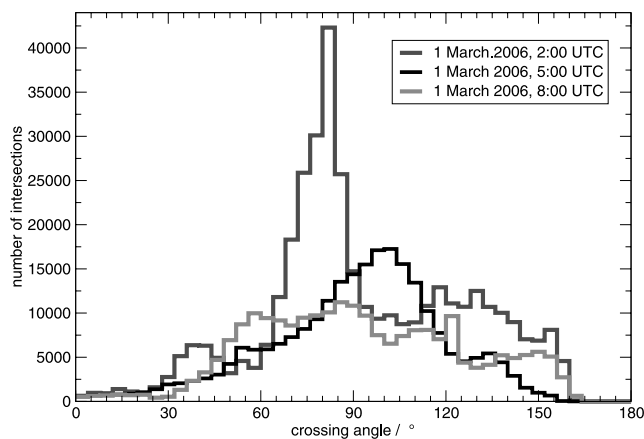


Figure 10. Crossing angle between the intersecting slant paths. The number of intersections within a 4° interval is given.

tions will also not provide reliable information. One way to estimate the quality of a reconstructed field is therefore to compute the number of slants and their intersections per grid cell using the same grid as the reconstruction. These 3D fields give a good impression of the spatial coverage. Figure 9 shows the horizontal (top) and vertical (bottom) projection of the slants per grid cell (left) and the intersections per grid cell (right) computed for a 40 km grid, i.e., a horizontal grid spacing of 40 km and a vertical spacing of 500 m. The horizontal projection shows the sum of all data within each vertical column from the ground level up to 12 km, the vertical projection gives the sum of all voxels in E-W direction. The inhomogeneous horizontal distribution of slant paths (Figure 9a) leads to the formation of clusters with a rather high density of slants per voxel surrounded by sparsely populated regions. The intersections per voxel (Figure 9b) are even more clustered. The intersection points of a given slant path with its neighbors are consequently not homogeneously distributed along the whole path but concentrated in several limited sections.

[35] There are also significant differences in the vertical profiles of the slant paths and their intersection points. The density of slants (Figure 9c) shows maximum values in the boundary layer which become slightly diluted at higher altitudes. In contrast, there are little intersection points near the surface layer (below 2000–3000 m in Figure 9d) but an increasing density at higher altitudes above ~ 4000 m. One could expect that most slant paths proceed almost vertically through the atmosphere as the GPS satellites are high above Earth's surface. But this is not true. Figure 4a shows that the probability for finding a satellite less than 40° above the horizon is much higher than finding it above this elevation. This becomes obvious if one looks at the satellite orbit from the local horizon system of the GPS station where each GPS satellite rises and sets twice a day (see Figure 5). According to Figure 4a, there is a large number of slant paths which propagate large distances through the lower part of the troposphere. Therefore, the information is present but it is not possible to make use of it as there are not enough stations nearby which would provide additional intersecting raypaths. Slant paths with an elevation above 10° cover only a horizontal distance up to 50 km before they leave the

troposphere at an altitude of ~ 10 km. To reveal the information about the vertical structure of the troposphere there must be a neighbored station within ~ 30 km. Furthermore, the reconstruction must use a grid with a horizontal spacing well below 50 km. The situation improves at higher altitudes where slants from distant stations result in more intersections and cover an increasing angular range.

[36] The currently available GPS network provides a highly inhomogeneous distribution of the slants and the intersection points as well. Only sparse data are available in northern and south eastern Germany. Even some central parts of Germany are not covered very well. The latter would require a more dense GPS network in Germany with interstation distances between 20 km and 30 km. The situation at the boundaries could considerably be enhanced by making use of GPS slant data from neighbored countries. There are dense GPS networks in central Europe which already provide a combined data set of IWV data ([Elgered *et al.*, 2004], E-GVAP, <http://egvap.dmi.dk>) and a comparable set of slant data should be available in near future.

[37] The inhomogeneous distribution may lead to severe problems during the tomographic reconstruction. Regarding a single slant path there are only few intersections with other slant paths which can be used to distribute the integral value along the ray path. If there is a large number of intersections in a very limited region some reconstruction techniques tend to concentrate a large fraction of the integral value in this region. The reconstruction may become divergent and result in some “hot spots” in an almost empty grid. Using the reconstruction technique described in section 3.1 the high density of intersection points near Berlin leads to severe artifacts in the reconstructed field. A more homogeneous network would be required which results in a smooth vertical distribution of intersection points.

[38] It must be pointed out that only the GPS data are regarded in this work. A real tomographic reconstruction algorithm would make use of meteorological observations and model constraints which reduce the degrees of freedom drastically. Meteorological observations and possibly data from numerical weather models can be used to define a realistic initial field for the reconstruction and provide additional information which are used during the reconstruction procedure and which stabilise this process. Reliable tomographic results were obtained on the basis of GPS networks with a receiver density comparable to the German network [Troller *et al.*, 2006a, 2006b].

[39] Nevertheless, the considerations made in this work are important to estimate the information provided by the GPS data and to separate it from the information introduced by other meteorological observations or model constraints. Especially the initial vertical profiles depend strongly on the surface data and possibly on models describing the vertical structure of the troposphere which are used as constraint by the reconstruction. It must be carefully checked if the reconstructed profiles are really obtained from the GPS observations or if they are an “artifact” of the model constraints or initialization.

4. Conclusion

[40] The temporal and spatial distribution of GPS slant observations available within 3 days in March 2006 was

investigated with respect to a tomographic reconstruction of the humidity field above Germany. The GPS observations were used to quantify the information which can be expected in a certain region at a certain time. This was done from a geometric point of view considering only the slant paths through the atmosphere and their intersections but without regarding the path delays and their uncertainties. At the current configuration level of the GPS networks is the spatial covering fairly incomplete and it is initially necessary to identify the regions where input from the GPS slant data can be expected. Validating the quality of the GPS data is subject to further work.

4.1. Temporal Variations

[41] The number of visible GPS satellites and their positions in the local horizon system of a GPS station show strong temporal variations. Consequently, the number of slant data available in a given period varies by a factor of about 2. The variations become even more pronounced if slant paths with low elevations within smaller periods are considered. The data of consecutive periods may in such cases change by more than a factor of 5. The number of intersection points and so the information fluctuates more significantly by nearly 1 order of magnitude. This is also true for the spatial distribution. Regions covered very well in one period may receive little GPS input in the next period. The quality of the humidity fields reconstructed from these data will therefore be widely different. High-quality reconstructions may be followed by a situation which allows no reconstruction at all. This behavior must be kept in mind if an operational 3D water vapor monitoring system is planned.

4.2. Spatial Variations

[42] Equally important as the temporal variation is the spatial variation within a given distribution at a certain time. This distribution and with it the spatial coverage of the atmosphere depends to a large extent on the receiver arrangement of the GPS networks. The networks are not designed for atmosphere sounding applications and optimal results can therefore not be expected. The density of slant paths shows a very inhomogeneous horizontal distribution. Most parts of Germany are covered fairly well by GPS observations with some limited regions which are crossed by a large number of slant paths and other regions with very little data. The intersection points are even more clustered showing spots with a high concentration of intersections in a sparsely populated environment. The vertical distribution displays some characteristic features which are important to estimate the vertical resolution which can be obtained from the GPS slant data. While the density of slant paths is maximal near the ground and decreases with height the density of intersections behaves contrarily. There are little intersections in the boundary layer and the vertical structure cannot be reconstructed reliably in this region. The situation improves above ~ 4 km where a rather high number of intersections can be expected.

4.3. Spatial Resolution

[43] Another important parameter is the resolution of the grid used to reconstruct the humidity field. Its horizontal resolution must be adjusted to the receiver density of the

GPS networks. If the resolution is too high a large number of grid cells will be crossed by very little slant paths and contain virtually no intersection points. On the contrary, to take advantage of the information on the vertical resolution provided by the slant data is only possible if a large number of slant paths propagates to several horizontally neighbored grid cells. This requires a rather small grid spacing, i.e., a high spatial resolution. In the current situation with a horizontal grid spacing of 50–60 km about two thirds of the observed slants can be used to enhance the vertical resolution of the humidity fields. As a consequence, the remaining one third of the slants cannot contribute any information about the vertical structure of the atmosphere. A much better resolved grid would be required to utilise the information hidden in these slant paths.

4.4. Complemental Observations

[44] Summarising, the currently available GPS stations in Germany are not sufficient to reconstruct the entire 3D water vapor field above Germany exclusively from GPS data. The inhomogeneity of the slant path distribution and especially the distribution of intersection points is a severe problem for the tomographic reconstruction. The distances between neighbored GPS stations are too large to obtain a sufficient number of intersection points and to locate the slant delay information reliably. Especially the absence of slant path intersections in the boundary layer has an adverse effect on the reconstruction of vertical profiles. However, it could be demonstrated in numerous experiments that the GPS tomography is able to provide reliable spatially resolved humidity information. But this requires the utilization of additional meteorological observations and some model constraints. Combining the usually available meteorological observations with the GPS slant data in the tomographic reconstruction helps to stabilize the reconstruction algorithm and leads in most cases to more reliable results. The results obtained in this work are important to separate the information provided by the GPS slant data from the information contributed by the meteorological observations. As stated above, there will always be some regions or some periods where little GPS data are available and where the field obtained from the meteorological observations remains virtually unchanged. It is therefore important to identify such regions or periods before the impact of the GPS data is validated.

4.5. Outlook

[45] The situation in March 2006 with only 135 GPS processed stations in Germany is not an optimal constellation for the GPS tomography. But the GPS observations have some very promising features which show the great potential of this technique. One of the most severe problems of the GPS tomography is the reconstruction of the boundary layer. This requires a large number of slant paths with low elevations propagating through large parts of the lower atmosphere. These slant data are already available. The maximum of the distribution is located at very low elevations near $\varepsilon = 11^\circ$, 44.5% of the observed slant paths have elevations below 30° . These data carry considerable information about the boundary layer but to get at this information additional slant observations would be required which constitute a sufficient number of intersections. In parallel,

the grid must be refined to locate the information in different cells. To meet these requirements additional stations must be installed. The strong anisotropy of the azimuth distribution could be used to optimize existing networks for meteorological applications. To make best use of additional stations they could be placed in such a way that each station is located within the northeast or northwest of another station. Most slants with low elevation angles are concentrated in these directions and information about the lower part of the troposphere could most easily be obtained, if the neighboring stations were placed in these directions.

[46] The efforts to optimize the ground receiver networks will in the next years be supported by the extension of the Global Navigation Satellite Systems (GNSS). After the European Galileo system is operational and the Russian Glonass is renewed about 90 GNSS satellites will be available, 20 to 30 of them visible at any time. This will triple the GPS observations available today and the number of intersection points will approximately increase according to a square law. Future GNSS-based atmosphere sounding systems will achieve temporal and spatial resolutions which are far beyond the situation described in this work.

References

- Bender, M., and A. Raabe (2007), Preconditions to ground-based GPS water vapour tomography, *Ann. Geophys.*, 25(8), 1727–1734.
- Bevis, M., S. Businger, T. A. Herring, C. Rocken, R. A. Anthes, and R. H. Ware (1992), GPS meteorology: Remote sensing of atmospheric water vapor using the global positioning system, *J. Geophys. Res.*, 97(D14), 15,787–15,801.
- Bevis, M., S. Businger, S. Chiswell, T. A. Herring, R. A. Anthes, C. Rocken, and R. H. Ware (1994), GPS meteorology: Mapping zenith wet delays onto precipitable water, *J. Appl. Meteorol.*, 33(3), 379–386, doi:10.1175/1520-0450.
- Businger, S., S. R. Chiswell, M. B. J. Duan, R. A. Anthes, C. Rocken, R. H. Ware, M. Exner, T. VanHove, and F. S. Solheim (1996), The promise of GPS in atmospheric monitoring, *Bull. Am. Meteorol. Soc.*, 77(1), 5–18, doi:10.1175/1520-0477.
- Dick, G., G. Gendt, and C. Reigber (2001), First experience with near real-time water vapor estimation in a German GPS network, *J. Atmos. Solar Terr. Phys.*, 63(12), 1295–1304.
- Elgered, G., H.-P. Plag, H. van der Marel, S. Barlag, and J. Nash (2004), Exploitation of ground-based GPS for climate and numerical weather prediction applications, *Final report*, Working Group I of COST Action 716, Brussels. (Available at http://www.oso.chalmers.se/kge/cost716.html/COST716_FR_Oct27.pdf)
- Flores, A., J.-G. de Arellano, L. P. Gradinarsky, and A. Rius (2001), Tomography of the lower troposphere using a small dense network of GPS receivers, *IEEE Trans. Geosci. Remote Sens.*, 39(2), 439–447.
- Gendt, G., G. Dick, and W. Söhne (1999a), GFZ Analysis Center of IGS—Annual report 1998, in *1998 Technical Reports*, edited by K. Gowey, R. Neilan, and A. Moore, pp. 79–87, IGS Central Bureau, Pasadena, Calif.
- Gendt, G., P. Fang, and J. F. Zumberge (1999b), Moving IGS products towards real-time, in *1999 Technical Reports*, edited by K. Gowey, R. Neilan, and A. Moore, pp. 391–404, IGS Cent. Bur., Jet Propul. Lab., Pasadena, Calif.
- Gendt, G., G. Dick, C. Reigber, M. Tomassini, Y. Liu, and M. Ramatschi (2004), Near real time GPS water vapor monitoring for numerical weather prediction in Germany, *J. Meteorol. Soc. Jpn.*, 82(1B), 361–370.
- Gradinarsky, L. P., and P. Jarlemark (2004), Ground-based GPS tomography of water vapor: Analysis of simulated and real data, *J. Meteorol. Soc. Jpn.*, 82(1B), 551–560.
- Heise, S., J. Wickert, G. Beyerle, T. Schmidt, and C. Reigber (2006), Global monitoring of tropospheric water vapor with GPS radio occultation aboard CHAMP, *Adv. Space Res.*, 37(12), 2222–2227, doi:10.1016/j.asr.2005.06.066.
- Kak, A. C., and M. Slaney (1999), *Principles of Computerized Tomographic Imaging*, 327 pp., Inst. of Electr. and Electron. Eng., New York.
- Kunitsyn, V. E., and E. D. Tereshchenko (2003), *Ionospheric Tomography*, 260 pp., Springer, Berlin.
- Kursinski, E. R., G. Hajj, J. Schofield, R. Linfield, and K. Hardy (1997), Observing Earth's atmosphere with radio occultation measurements using the Global Positioning System, *J. Geophys. Res.*, 102(D19), 23,429–23,465.
- Natterer, F. (2001), *The Mathematics of Computerized Tomography, Classics Appl. Math.*, vol. 32, 222 pp., Soc. of Indust. and Appl. Math, Philadelphia, Pa.
- Santerre, R. (1991), Impact of GPS satellite sky distribution, *Manuscr. Geod.*, 16(1), 28–53.
- Seko, H., S. Shimada, H. Nakamura, and T. Kato (2000), Three-dimensional distribution of water vapor estimated from tropospheric delay of GPS data in a mesoscale precipitation system of the baiu front, *Earth Planets Space*, 52(11), 927–933.
- Stolle, C., S. Schlüter, M. Heise, C. Jacobi, N. Jakowski, and A. Raabe (2006), A GPS based three-dimensional ionospheric imaging tool: Process and assessment, *Adv. Space Res.*, 38(11), 2313–2317, doi:10.1016/j.asr.2006.05.016.
- Subbarao, P. M. V., P. Munshi, and K. Muralidhar (1997), Performance of iterative tomographic algorithms applied to non-destructive evaluation with limited data, *NDT E Int.*, 30(6), 359–370.
- Troller, M., A. Geiger, E. Brockmann, J.-M. Bettems, B. Bürki, and H.-G. Kahle (2006a), Tomographic determination of the spatial distribution of water vapor using GPS observations, *Adv. Space Res.*, 37(12), 2211–2217.
- Troller, M., A. Geiger, E. Brockmann, and H.-G. Kahle (2006b), Determination of the spatial and temporal variation of tropospheric water vapour using GPS networks, *Geophys. J. Int.*, 167(2), 509–520.
- Ware, R., C. Alber, C. Rocken, and F. Solheim (1997), Sensing integrated water vapor along GPS ray paths, *Geophys. Res. Lett.*, 24(4), 417–420, doi:10.1029/97GL00080.
- Ware, R. H., et al. (2000), Suominet: A real-time national GPS network for atmospheric research and education, *Bull. Am. Meteorol. Soc.*, 81(4), 677–694, doi:10.1175/1520-0477.
- Wickert, J., et al. (2007), Ground and space based GPS atmospheric sounding: Brief overview and examples, in *Proceedings of the INTAR Colloquium*, edited by V. K. Anandan, J. Roettger, and D. N. Rao, pp. 1–10, Natl. Atmos. Res. Lab., Gadanki, India.
- Wickert, J., et al. (2008), CHAMP, GRACE, SAC-C, TerraSAR-X/TanDEM-X: Science results, status and future prospects, paper presented at GRAS SAF Workshop on Applications of GPS Radio Occultation Measurements, Eur. Cent. for Medium-Range Weather Forecasts, Reading, U. K.
- Wickert, J., et al. (2009), GPS radio occultation: Results from CHAMP, GRACE and FORMOSAT-3/COSMIC, *Terr. Atmos. Oceanic Sci.*, in press.
- Zumberge, J. F., M. B. Hefflin, D. C. Jefferson, M. M. Watkins, and F. H. Webb (1997), Precise point positioning for the efficient and robust analysis of GPS data from large networks, *J. Geophys. Res.*, 102(B3), 5005–5018, doi:10.1029/96JB03860.
- Zus, F., M. Grzeschik, H.-S. Bauer, V. Wulfmeyer, G. Dick, and M. Bender (2008), Development and optimization of the IPM MM5 GPS slant path 4DVAR system, *Meteorol. Z.*, 17(6), 867–885.

M. Bender, G. Dick, M. Ge, G. Gendt, M. Ramatschi, M. Rothacher, and J. Wickert, Helmholtz-Zentrum Potsdam, Deutsches GeoForschungs-Zentrum, Telegrafenberg, D-14473 Potsdam, Germany. (bender@gfz-potsdam.de)

A. Raabe and G. Tetzlaff, Institut für Meteorologie, Universität Leipzig, D-04103 Leipzig, Germany.